

PFC/JA-86-1

A Gyrotron with a Minimum Q Cavity

H. Saito*, K. Kreischer, B. G. Danly, T. M. Tran**
and R. J. Temkin

January 1986

Massachusetts Institute of Technology
Plasma Fusion Center
Cambridge, Massachusetts

Permanent Address:* Institute of Space and Astronautical Science,
Tokyo, Japan

** CRPP, Association Euratom-Confederation Suisse,
EPFL, Lausanne, Switzerland

Submitted for publication in: International Journal of Electronics

Abstract

In order to reduce the wall loading of a gyrotron cavity, a gyrotron with a minimum Q cavity is proposed and experimentally tested at 140 GHz. The minimum Q is defined as Q ($Q_{\min} = 4\pi(L/\lambda)^2$, where L and λ are the effective cavity length and the wavelength. A nonlinear up-taper, the radius of which gradually changes with respect to the axial direction, is used to minimize the reflection at the output taper of the open resonator. The detailed performance is investigated by means of self-consistent gyrotron theory. It is found that the electron beam significantly modifies the RF axial field profile in comparison with the cold cavity profile through the interaction between the electrons and the RF field. The maximum experimental efficiency of 37 % is achieved at 150 kW and is compared with the results of self-consistent gyrotron theory. These theoretical and experimental results show the feasibility of the minimum Q cavity, especially for high power and high frequency gyrotrons.

1. Introduction

Recently, gyrotron research and development has progressed rapidly (Felch, ed. 1985). In particular, significant progress has been made over the last decade in high power gyrotrons that can be used for electron cyclotron resonance heating (ECRH) of fusion plasmas. As fusion devices become larger and operate at higher magnetic fields, it will be necessary to develop cw gyrotrons that operate at both higher frequencies and at higher powers.

The authors have developed a 200 kW, 140 GHz pulsed gyrotron (Kreischer et al. 1984), and are developing a 1 MW, 120 GHz gyrotron (Kreischer et al. 1985). One of the technological constraints of high frequency and high power gyrotrons is wall loading of the cavity due to ohmic losses. Typically, an average wall loading of about 2 kW/cm^2 is the maximum value of tolerable wall loading for presently available cooling technology. To decrease the wall loading, it is necessary to decrease the magnitude of electric field in the cavity. Let Q be the quality factor of the cavity. The power balance condition gives $Q = U\omega/P$, where U , P , and ω denote the stored energy of the cavity, the output power, and the frequency, respectively. For a fixed output power P at the frequency ω , we have to decrease Q in order to reduce the stored energy or the electric field in the cavity. Alternatively, for a fixed wall loading, the output power could be increased as Q is reduced.

Generally, the diffractive Q value of an open resonator is expressed as $Q = 4\pi(L/\lambda)^2(1-R)^{-1}$ (Vlasov et al. 1969, Temkin 1981), where L is the cavity length, λ is the wavelength, and R is the cavity reflectivity coefficient at the output taper. This formula shows that Q has a minimum

value $Q_{\min} = 4\pi(L/\lambda)^2$ for a fixed cavity length and frequency.

To achieve high efficiency with a gyrotron, the cavity length must be optimized using nonlinear gyrotron theories (Nusinovich and Erm 1972, Danly and Temkin 1986). Therefore, the reflection R must be reduced in order to decrease Q while at the same time the cavity length must remain optimized.

To make this point clear, we use the nonlinear theory of a gyrotron with a Gaussian axial field profile (Nusinovich and Erm 1972), which has been exploited for the wide range of gyrotron designs (Kreischer et al. 1984, Saito et al. 1985). This theory shows that the perpendicular efficiency η_{\perp} can be expressed in terms of three parameters (see Eq.(1), Sec. 2): the normalized cavity length μ , the normalized RF field magnitude F , and the frequency detuning Δ . Figure 1 shows the equicontour curves η_{\perp} after optimization with respect to the detuning parameter. The average ohmic losses in the cavity walls are also shown for the TE_{031} mode, with the conductivity $\sigma = 5 \times 10^7 (\Omega m)^{-1}$, and a frequency of 140 GHz. Using the power balance condition, the lines of $Q/Q_{\min} = 2.5$ and 1 are shown in Fig.1 for $P = 100$ kW. The point A corresponds to the gyrotron with a $Q = 1515$ cavity, which we reported previously (Kreischer et al. 1984). On the other hand, the point B corresponds to the present gyrotron with minimum Q value. As is seen in Fig.1, the minimum Q gyrotron at the point B has a slightly higher efficiency and a lower field strength F by a factor 1.4, compared with the gyrotron at the point A for the same output power and frequency. The wall loading is proportional to F^2 , so this reduction of F means a reduction of the wall loading by a factor of two. As will be discussed below, the RF field of a cavity with low reflectivity is not exactly a Gaussian profile and also is modified by the electron beam. Therefore, the above discussion is an approxi-

mate, but useful, estimate of the performance of a minimum Q gyrotron.

In gyrotrons, resonators with a linear up-taper are widely utilized (Fliflet et al. 1982, Kreischer et al. 1984, Saito et al. 1985). However, the sudden change of the cavity radius in such a linear up-taper induces reflection of the radiation and results in the increase of the cavity Q. A small linear taper (less than 1 degree) could be used to reduce this reflection, but this would require very long tapers. In this research, we use a nonlinear up-taper in order to obtain a gyrotron with a minimum Q cavity ($Q/Q_{\min} = 1$). This allows a smooth transition from the cavity to the output waveguide in a reasonable axial distance.

In such gyrotrons with very low reflectivity, the effect of the cavity boundary (which can fix the RF field profile with respect to the axial direction) may be very weak. Instead, the interaction between the electron beam and the RF field may modify significantly the axial RF field profile, as compared with the cold cavity profile without the electron beam. This means that it is necessary to analyze self-consistently the interaction between the electrons and the RF field, solving simultaneously the electron equation of motion and the wave equation. Such self-consistent theories of gyrotrons have been developed (Bratman et al. 1973, Bratman et al. 1975, Flyagin et al. 1977, Charbit et al. 1981, and Fliflet et al. 1982).

Fliflet and coworkers (Fliflet et al. 1982) carried out a 35 GHz gyrotron experiment with a low Q (~ 210) cavity and compared the experimental results with those of a self-consistent gyrotron theory. However, their cavity had a 36 degree linear up-taper which would be expected to give a very high reflectivity, and the cavity was very short ($L/\lambda \sim 2.7$). This fact means that Q/Q_{\min} was large (~ 2.3) and the self-consistent effect on the RF field

profile is less dominant than would be expected for $Q/Q_{\min} \sim 1$. Thus, low Q cavities represent a different physical situation than minimum Q cavities. The need for a self-consistent theory increases as Q/Q_{\min} approaches unity, and does not depend on the absolute value of Q .

In this work, we realize the gyrotron with a minimum Q cavity ($Q/Q_{\min} = 1$) by using the nonlinear up-taper and analyze the performance by means of the self-consistent theory. It is found that the self-consistent effect modifies significantly the RF field profile and the gyrotron performance. Experimentally, we achieved maximum efficiency of 37%, maximum output power of 195 kW at 127 GHz, with this minimum Q gyrotron. In Sec.2, we describe the design of the minimum Q cavity and the results of calculations. Section 3 deals with the experimental results. Finally, discussion and the conclusions can be found in Sec.4.

2. Design and Calculation of Minimum Q Gyrotron

2-1. Model of Gyrotron

In this section, the model used in this study to describe the interaction between the beam and RF field will be described. The total efficiency of the gyrotron interaction can be written as $\eta_T = \eta_{\perp} \eta_{e\perp} \eta_Q$, where η_{\perp} is the efficiency of energy extraction from the perpendicular component of the beam, $\eta_{e\perp}$ is the amount of beam power in the perpendicular component, and η_Q is the reduction in efficiency due to ohmic loss in the cavity walls. If $\beta_{\perp} = v_{\perp}/c$, where v_{\perp} is the perpendicular velocity of the electrons, and $\gamma = 1 + V_c/511$, where V_c is the cathode voltage in kV, then $\eta_{e\perp} = 0.5\beta_{\perp}^2/(1 - \gamma^{-1})$. The reduction in efficiency due to cavity wall loss can be shown to be quite small ($0.8 \lesssim \eta_Q \lesssim 1$) in high power gyrotrons where $Q_D \ll Q_{OHM}$. In the theoretical calculations presented here, η_Q has been set to one for simplicity.

In order to determine η_{\perp} the nonlinear interaction between the beam and RF fields within the cavity must be analyzed. Studies have shown (Nusinovich and Erm 1972, Danly and Temkin 1986) that this interaction can be represented by generalized differential equations that describe the evolution of the energy of the electrons, and their phase with respect to the field. A detailed derivation of these equations can be found in the reference (Danly and Temkin 1986). By considering the RF field component which is synchronous with the oscillatory motion of the electrons, these equations can be expressed in terms of slow time variables. These studies also show that when the beam is weakly relativistic ($n\beta_{\perp}^2 \ll 1$, $n =$ harmonic number), η_{\perp} can be expressed in terms of the following three parameters for a given axial RF field profile:

$$\begin{aligned}
\mu &= \pi(\beta_{\perp}^2/\beta_{\parallel})(L/\lambda) \\
\Delta &= (2/\beta_{\perp}^2)(1-n\omega_c/\omega) \\
F &= (E_0\beta_{\perp}^{n-4}/B_0c)(n^{n-1}/2^{n-1}n!)J_{m+n}(k_{\perp}R_e)
\end{aligned}
\tag{1}$$

In these equations $\beta_{\parallel} = v_{\parallel}/c$, where v_{\parallel} is the parallel electron velocity, λ is the wavelength, and n is the harmonic number. The length L characterizes the width of the axial field profile. The parameter Δ indicates the detuning between ω_c , the initial cyclotron frequency, and ω , the oscillation frequency. The coupling strength between the beam and RF field is represented by the parameter F . All dimensioned variables are assumed to be in MKS units unless otherwise noted. The Bessel function J_{m+n} is a measure of the coupling of the RF field to the beam at radius R_e . The choice of signs in the subscript depends on the direction of azimuthal rotation of the mode. The magnetic field is given by B_0 , and $k_{\perp} = v_{mp}/R_0(z)$, where R_0 is the cavity radius, and v_{mp} is the p th nonvanishing root of $J_m'(x) = 0$ and describes the transverse structure of the RF field. The electric field of the TE_{mp} mode is given by

$$\begin{aligned}
\vec{E} &= \text{Re}\{E_0 k_{\perp} [J_m'(k_{\perp}r) \hat{\theta} + (im/k_{\perp}r) J_m(k_{\perp}r) \hat{r}] \\
&\quad \times f(z) \exp[i(\omega t - m\theta)] \}
\end{aligned}
\tag{2}$$

The axial dependence of the RF field in the resonator is given by the complex profile function

$$f(z) = |f(z)| \exp\{-i\psi(z)\}, \tag{3}$$

where $k_{\perp} |f(z)| = 1$ at its maximum value.

We have used the following three models for the RF axial field profile:

1) A simplified Gaussian Profile Model in which the RF axial field profile is assumed to be a Gaussian extending from $-\sqrt{3} L/2$ to $\sqrt{3} L/2$:

$$f(z) = \exp\{-(2z/L)^2\}/k_{\perp} , \quad (4)$$

where E_0 is the amplitude and L is the width of the profile. The phase is assumed not to change spatially. The efficiency η_{\perp} , which is obtained from the slow-time-scale calculation of the electron motion, is presented in the references Nusinovich and Erm 1972, and Danly and Temkin 1986. 2) A Cold Cavity Profile Model in which the cold cavity RF profile function is calculated by numerically solving the homogeneous wave equation. We utilized a code similar to that described by Fliflet and coworkers (Fliflet and Read 1981) to obtain the cold cavity profile. The slow-time-scale equations for the electron motion are then solved to obtain the gyrotron efficiency. 3) A Self-Consistent Profile Model in which the RF axial field profile function satisfies a wave equation with the high frequency electron beam current appearing as a source. The wave equation is solved simultaneously with the electron equation of motion. For this model, we employed the self-consistent field code developed by Fliflet and coworkers (Fliflet et al. 1982).

2-2. Cavity Design

The design of the minimum Q cavity was first performed by means of a simplified Gaussian profile model. The effective cavity length L which characterizes the width of the axial field profile is obtained by using the cold cavity profile. We show the design in this section. The detailed gyrotron performance was then tested by means of the self-consistent profile model which will be described in Sec.2-3.

The simplified Gaussian profile model gives the efficiency η_{\perp} optimized with respect to the detuning as a function of F and μ , in Fig.1. The power balance condition yields (Kreischer et al. 1985) a relation between μ , F and R

$$\mu = 2155F^2(1 - 0.5\beta_{\perp}^2\Delta)^2/C_D \quad (5)$$

where

$$C_D = 2P(\text{MW})/[C_{mp}^2(v_{mp}^2 - m^2)\beta_{\perp}^7\gamma^2\alpha(1-R)] \quad (6)$$

Here $\alpha = \beta_{\perp}/\beta_{\parallel}$, and $C_{mp} = J_m(v_{mp})/J_{m \pm n}(k_{\perp}R_e)$. In Fig.1, this equation has been plotted for $Q/Q_{\min} = 2.5$ and 1, assuming the output power $P = 100$ kW, and $\beta_{\perp}^2\Delta = 0.1$. Under the condition of a constant output power, an optimum cavity length (μ) is required for high efficiency. This graph indicates that the Q/Q_{\min} value should approach unity in order to reduce the field magnitude in the cavity and maintain high efficiency.

For a given cavity shape, the cold cavity field profile is calculated, and the Q value is found. The cold cavity field profile gives an equivalent cavity length for the best-fitted Gaussian profile. Using the Q value and the effective cavity length, Q/Q_{\min} or $(1-R)^{-1}$ are obtained. We optimized the cavity shape so that the efficiency becomes high and Q/Q_{\min} approaches unity in Fig.1. We tried several types of cavities including cavities with linear and nonlinear (square, cubic, and quartic) up-tapers. Linear up-tapers induce strong reflection due to the sudden change of the radius, even if the taper angle is very small ($< 1^\circ$). We found that nonlinear up-tapers, which have gradually varying radius with respect to the axial direction, are very effective in reducing the reflection.

The above-mentioned iterative design yielded one of the optimized gyrotron cavities shown in Fig.2. The cavity consists of the 1° linear down-taper, the straight section, and the cubic up-taper, the radius of which increases as the cubic function with respect to the axial direction. The cubic up-taper is 4.5cm in length and connects smoothly with the straight section and the extension linear taper with 2° angle. For the TE₀₃₁ mode, the cold cavity resonance frequency is 139.58 GHz, and $Q = 1150$.

For the cold cavity model, the field amplitude $|f(z)|$ normalized by the peak value and the phase of the cold cavity profile are shown in Fig.3, by the broken lines. The field amplitude peaks near the junction between the straight section and the up-taper, because the cubic up-taper requires some axial distance over which the change of the radius is enough to reflect the wave. Also, the wave reflection is widely distributed in some axial distance and the field amplitude shows the very gradual decrease in the up-taper. The phase varies gradually in the straight section and starts linearly changing in the output section. The effective length L characterizing the width of the axial field profile is evaluated by fitting a Gaussian profile to the $f(z)$ function shown in Fig.3, and we find $\mu \approx 17$ in Eq.(1). This value yields $Q_{\min} \approx 1100$ and our cavity satisfies $Q/Q_{\min} \approx 1$. Roughly, this cavity corresponds to the point B for $P = 100$ kW, and Fig.1 shows $\eta_1 = 70\%$ and $F = 0.115$, which corresponds to a wall loading of 1.4 kW/cm^2 , assuming the conductivity of the cavity wall is $\sigma = 5.0 \times 10^7 \text{ } (\Omega\text{m})^{-1}$ (annealed OFHC copper).

2-3. Self-consistent Calculation

The self-consistent calculations are performed for the cavity shown in Fig.2. We used the self-consistent computation code by Fliflet and

coworkers (Fliflet et al. 1982). Figures 3 and 4 show the self-consistent RF field profiles by the solid lines. The field amplitude $|f(z)|$ is normalized to its peak value. In Fig.3, the beam current is fixed at $I = 5A$, and the magnetic field varies from the optimum value of $B_0 = 5.37$ T to the nonoptimum value of $B_0 = 5.40$ T. In Fig.4, we show the field profiles for the fixed magnetic field $B_0 = 5.42$ T, varying the current from the optimum value $I = 2A$ to the nonoptimum value of $I = 5A$.

The equicontour plots of the frequency (Fig.5), and the total efficiency η_T (Fig.6) are shown in the plane of the magnetic field B_0 and the current I . The self-consistent frequency is always higher than the cold cavity frequency, and increases as both the magnetic field and the current increase. The maximum total efficiency is 60% (the perpendicular efficiency $\eta_{\perp} = 87\%$) and is remarkably high.

The self-consistent field profile which gives the maximum efficiency 60% at $I = 5A$, $B_0 = 5.37T$, and the corresponding profile of the efficiency are shown in Fig.3. For comparison, the profile of the efficiency corresponding to the cold cavity field profile is also shown in Fig.3 by the broken line, for the same current and magnetic field. In both models, the spatial profile of the efficiency rises up quickly in the straight section and saturates once, and then rises again a little. After that, the small periodic fluctuations can be seen. It is observed that the self-consistent field amplitude has the corresponding periodic fluctuation in the up-taper. This interaction is due to the periodic bunching in the electron phase of the cyclotron motion, and modifies the self-consistent field profile. The nonlinear taper, the radius of which varies gradually, enhances the interaction between the RF field and the electron in the wide range of the up-taper. As the consequence of this multi-stage

interaction, the maximum efficiency increases by more than 10%, compared to what the simplified Gaussian profile model predicts. It is found that the peak position of the self-consistent field profile is at lower z and the field width is narrower, compared to the cold cavity profile. Figure 3 shows that, for a fixed current, this effect is enhanced as the magnetic field increases away from the optimum value. It has been found (Fliflet et al. 1982, Saito et al 1986) that the RF field in a gyrotron cavity consists of a forward and backward travelling waves of the waveguide mode, and two electron cyclotron waves, and that the interaction between the electrons and the backward wave is enhanced as the magnetic field increases. This interaction with the backward travelling wave pushes back the RF axial field profile (Saito et al. 1986).

This narrowing effect on the field profile due to the self-consistent effect means the increase in the effective Q/Q_{\min} or the reflective coefficient of the cavity. For a given output power, the self-consistent effect increases the RF field magnitude, compared to the cold cavity field profile. Figure 7 plots the RF field magnitude defined in Eq.(1) and the total efficiency η_T , which are optimized with respect to the magnetic field, as a function of the beam current I . The solid line and broken lines correspond to the self-consistent profile model, and the cold cavity profile model, respectively. For a fixed current, the self-consistent profile model gives the higher field magnitude F than the cold cavity profile model, by a factor 1.4. The efficiency of the self-consistent profile model is slightly higher than that of the cold cavity profile model.

Table 1 summarizes the calculated results of the minimum Q gyrotron, including the beam current, the output power, the field magnitude F , and

the efficiency for the fixed output 100 kW. The cold cavity profile model gives a smaller current, a smaller F value, and a higher efficiency, than the Gaussian profile model. This is consistent with the fact that the cold cavity profile is broader and the efficiency increases even in the up-taper section. However, the self-consistent effects narrow the profile as Figs.3, and 4 show, and the F value increases compared to the cold cavity profile model. Consequently, the F value of the self-consistent profile model for 100 kW output power is quite close to that of the Gaussian profile model. In the self-consistent profile model, however, the efficiency is higher and the current is smaller than the Gaussian profile model. The results with the peak efficiency are also shown in Table 1. The self-consistent profile model results indicate that 195 kW can be generated in the TE₀₃₁ mode consistent with an average wall loading of 2 kW/cm².

3. Experiment

3-1. Experimental Instruments

The minimum Q cavity shown in Fig.2 was electroformed. We measured the axial profile of the mandril radius and checked the dimensional accuracy. The cold cavity test was performed in reflection by using an IMPATT diode oscillator and a high sensitivity heterodyne receiver system (Woskoboinikow et al. 1985) The experimental cold cavity Q was 1300 ± 100 , which is in good agreement with the calculated value of 1150.

The cavity was inserted into the MIT gyrotron, which has been described previously (Kreischer et al. 1984). The main magnetic field is provided continuously by a Bitter coil. The cavity is connected with the electron gun through a gate valve and a beam tunnel. The electron gun produces an electron beam up to 10 A at 65 kV and operates with a 1-2 μ s. pulse. The gun is provided with its own magnetic coil so that the beam quality can be optimized.

The millimeter wave radiation after the cavity is propagated along an over-moded circular waveguide with 1.27 cm inner diameter; this waveguide also acts as the beam collector. The millimeter wave radiation is launched into free space through a motheye window. This motheye window has low reflection over a broad band of frequencies (Ma and Robinson, 1983). Two separate orthogonal pyramid arrays are cut by ultrasonic machinery on each side of the 7.1 mm thick fused quartz window. The period and the depth of the pyramid are designed to be 0.63 mm and 1.27 mm, which give a very good transmission performance between 120 and 240 GHz. The transmission coefficient was experimentally measured in free space and found to be ~98 % around 138 GHz.

Measurement of the gyrotron performance was made with several instruments including a video-diode, a calorimeter for power measurement, and a harmonic mixer system and a surface acoustic wave (SAW) dispersive line for precise frequency and line width measurement.

3-2. Experimental Results

The gyrotron cavity was designed for optimum operation at 140 GHz in the TE_{031} mode. It was found, however, that the optimum efficiency zone could not be investigated in this mode because of mode competition from the near TE_{231} mode. This mode competition effect has been previously observed at very high power levels (Kreischer et al. 1984). Therefore, we chose to investigate operation of the gyrotron in the TE_{421} mode at 127 GHz, a mode which is isolated and has no important mode competition effects. The previous discussion of self-consistent effects in the TE_{031} mode is also applicable to the TE_{421} mode. This follows because the gyrotron cavity properties are, to good accuracy, separable into the transverse and axial profiles. Although the TE_{031} and TE_{421} modes have very different transverse mode structure, the axial profiles are nearly identical. Since the self-consistent field effects in the present experiments primarily affect the axial field profile, the results in the TE_{421} mode provide a good test of a minimum Q cavity without the added complication of mode competition.

Figure 8 plots the total efficiency, output power field, and the optimum magnetic field as a function of the beam current. The beam voltage is 62.3 kV. The maximum efficiency is 37 % at 6.6 A, and the maximum output power is 195 kW. The efficiency and the output power are slightly higher than those of our previous cavity with a relatively high reflectivity (Kreischer et al. 1984). The efficiency is found to

peak at 6.6 A, about twice the current for peak efficiency in our previous experiment (Kreischer et al. 1984). This is consistent with the design goal of achieving optimum efficiency at 200 kW of output power in the present case vs. 100 kW in the previous design. In Fig.9, we show the corresponding results of the self-consistent theory, to compare with the experimental results in Fig.8. The self-consistent theory gives the maximum efficiency 60% at 5.5 A beam current, which is 1.6 times higher than the experimental maximum efficiency. Some of possible reasons for this discrepancy may be degradation due to cavity ohmic losses (i.e., $\eta_Q < 1$) and the finite thickness of the electron beam.

The starting current was measured for TE₄₂₁ mode. In Figure 10, the starting current as a function of the magnetic field is plotted, for V = 63.6 kV. The broken line shows the experimental result, and the solid lines are the self-consistent theory results for the fundamental axial mode $q = 1$, and the second higher mode $q = 2$. Because of the characteristics of our power supply, the experimental data along the high magnetic field side of the curve was determined by turning the mode on, while the data on the lower magnetic field side was determined by turning the mode off. The experimental result shows a good agreement with the theory ($q = 1$). The divergence of theory and experiment on the lower magnetic field side may be due to hysteresis effects in the hard excitation region of operation. The $q = 2$ mode was not observed and was probably suppressed by the $q = 1$ mode.

4. Discussions and Conclusions

One of the technological constraints of high power, high frequency gyrotrons is the wall loading due to the ohmic loss in the cavity. This wall loading can be reduced by using a cavity with a minimum diffractive Q value. This type of cavity (minimum Q cavity) has a very small reflection at the output taper, and the field magnitude in the cavity is reduced. We realized such a minimum Q cavity by using a nonlinear up-taper, the radius of which increases very gradually with respect to the axial direction. The feasibility of the minimum Q gyrotron has been demonstrated experimentally and a maximum efficiency of 37% at 150 kW, in the TE₄₂₁ mode at 127 GHz has been achieved. This efficiency is also slightly higher than that of our previous gyrotron (Kreischer et al. 1984).

A detailed theoretical analysis was performed by using the RF axial field profile of the cold cavity and the self-consistent field profile. The minimum Q gyrotron has several unique properties. The interaction between the electrons and the RF field occurs even over a up-taper section, because the radius of the nonlinear taper increases very slowly and the synchronous condition may be satisfied in the wide range of the up-taper. Consequently, the theoretical total efficiency reaches 60% (the perpendicular efficiency 87%), which is remarkably high. Secondly, the self-consistent effect of the interaction between the electrons and the RF field axial profile is dominant, because the geometrical structure of the cavity does not provide much reflection for the field. The self-consistent calculation is required to analyze the gyrotron performance. The most important effect is that the RF field axial profile gets narrower than the cold cavity profile, and the RF field magnitude increases for

the fixed current. This effect is caused by the interaction between the electrons and the backward travelling wave forming the cavity field profile together with the forward travelling wave of the waveguide mode. The self-consistent model indicates that output powers up to 200 kW can be generated in the TE_{031} mode at 140 GHz with an average ohmic wall loading less than 2 kW/cm^2 and a high efficiency.

Acknowledgements:

This research was conducted under U.S.D.O.E contract DE-AC02-78ET51013 and H. Saito was supported by Japan Society for Promotion of Science. The Francis Bitter National Magnet Laboratory and the National Science Foundation provided the high field magnet facilities.

References

- Bratman, V. L., Moiseev, M. A., Petelin, M. I., and Erm, R. E., 1973,
Theory of gyrotrons with a non-fixed structure of the high-frequency
field. Radiophys. Quant. Electron., 16, 474-480.
- Bratman, V. L., and Petelin, M. I., 1975, Optimizing the parameters of
high power gyromonotrons with RF field of non-fixed structure.
Radiophys. Quant. Electron., 18, 1136-1140.
- Charbit, P., Herscovici, A., and Mourier, G., 1981, A partly self-consistent
theory of the gyrotron. Int. J. Electron., 51, 303-330.
- Danly, B. G., and Temkin, R. J., 1986, Generalized nonlinear harmonic
gyrotron theory. Phys. Fluids (to be published).
- Felch, K., ed., 1985, Special issue on high-power microwave generation,
I.E.E.E. Trans. Plasma Science, PS-13, No.6.
- Fliflet, A. W., and Read, M. E., 1981, Use of weakly irregular waveguide
theory to calculate eigenfrequencies, Q values, and rf field
functions for gyrotron oscillators. Int. J. Electron., 51, 475-484.
- Fliflet, A. W., Read, M. E., Chu, K. R., and Seeley, R., 1982, A self-consistent
field theory for gyrotron oscillators: application to a low Q gyromonotron.
Int. J. Electron., 53, 505-521.
- Flyagin, V. A., Gaponov, A. V., Petelin, M. I., and Yulpatov, V. K., 1977,
The gyrotron. I.E.E.E. Trans. Microw. Theory and Tech., 25, 514-521.
- Kreischer, K. E., Schutkeker, J. B., Danly, B. G., Mulligan, W. J., and
Temkin, R. J., 1984, High efficiency operation of a 140 GHz pulsed
gyrotron. Int. J. Electron., 57, 835-850.
- Kreischer, K. E., Danly, B. G., Schutkeker, J. B., and Temkin, R. J., 1985,
The design of megawatt gyrotrons. I.E.E.E. Trans. Plasma Science,
PS-13, 364-373.

- Ma, J. Y. L., and Robinson, L. C., 1983, Night moth eye window for the millimetre and sub-millimetre wave region. *Optica Acta*, 30, 1685-1695.
- Nusinovich, G. S., and Erm, R. E., 1972, Efficiency of a CRM monotron with a Gaussian longitudinal distribution of high frequency fields. *Elektronnaya Tekhnika. Ser. 1, Elektronika SVCh*, 55-60.
- Saito, H., Danly, B. G., Mulligan, W. J., Temkin, R. J., and Woskoboinikow, P., 1985, A gyrotron with a high Q cavity for plasma scattering diagnostics. *I.E.E.E. Trans. Plasma Science*, PS-13, 393-397.
- Saito, H., Tran, T.M., Kreischer, K.E., and Temkin, R.J., 1986, Analytical treatment of linearized self-consistent theory for gyromonotron with nonfixed structure, Plasma Fusion Center Report, Massachusetts Institute of Technology, PFC/JA-86-2.
- Temkin, R.J., 1981, Analytical theory of a tapered gyrotron resonator., *Int. J. Inf. and Mm. Waves*, 2, 629-650.
- Vlasov, S. N., Zhislin, G. M., Orlova, I. M., Petelin, M. I., and Rogacheva, G. G., 1969, Irregular waveguides as open resonators. *Radiophys. Quant. Electron.*, 12, 972-978.
- Woskoboinikow, P., Cohn, D. R., Gerver, M., Mulligan, W. J., Post, R. S., Temkin, R. J., and Trulsen, J., 1985, A high frequency gyrotron diagnostic for instability studies on TARA. *Rev. Scientific Inst.*, 56, 914-916.

Table 1

Calculation Results of Minimum Q Gyrotron

	I(A)	$\eta_T(\%)$	P(kW)	F
Gaussian				
Model	3.4	48	100	0.115
Cold Cavity	3.1	51	100	0.09
Model	5.0*	56	180	0.105
Self-Consistent	2.9	54	100	0.11
Model	5.0*	60	195	0.145

V = 65 kV, $\alpha = 1.5$, TE₀₃₁ mode

* optimum efficiency point

Figure Captions

- Figure 1 Contours of perpendicular efficiency η_{\perp} in the plane of F and μ for a Gaussian profile model. Broken lines are for $Q/Q_{\min} = 2.5$ and 1, assuming $P = 100$ kW, 140 GHz, and TE_{031} mode. Average wall loading is also shown for $\sigma = 5 \times 10^7 (\Omega m)^{-1}$.
- Figure 2 Shape of minimum Q cavity using cubic up-taper.
- Figure 3 Axial RF field profiles and efficiency profiles of minimum Q gyrotron, for $I = 5$ A and the various magnetic field. The field amplitude $|f(z)|$ is normalized by its peak value. Solid and broken lines are self-consistent profile model and cold cavity profile model (C.C.), respectively. The top shows the position of the cavity.
- Figure 4 Axial RF field profiles for $B_0 = 5.42$ T and the various beam current. The field amplitude $|f(z)|$ is normalized by its peak value.
- Figure 5 Equicontour curves of oscillation frequency from self-consistent profile model, in the plane of beam current I and magnetic field B_0 . No oscillations occur in the hatched area.
- Figure 6 Contours of total efficiency η_T from the self-consistent profile model.
- Figure 7 Normalized RF field magnitude F and total efficiency η_T as functions of beam current I . Solid lines, and broken lines correspond to self-consistent profile model (S.C.), and cold cavity profile model (C.C.), respectively.
- Figure 8 Experimental results of output power P , total efficiency η_T , and optimized magnetic field B_{opt} , as functions of beam current I . TE_{421} mode and beam voltage 62.3 kV.

Figure 9 Theoretical results of output power P , total efficiency η_T , and optimized magnetic field B_{opt} , as functions of beam current I . Conditions are the same as Fig.8.

Figure 10 Starting current I_{st} as a function of magnetic field B_0 , for TE_{421} mode, and beam voltage 63.6 kV. Solid lines are theoretical data ($q=1$, and 2), and broken line is experimental data.

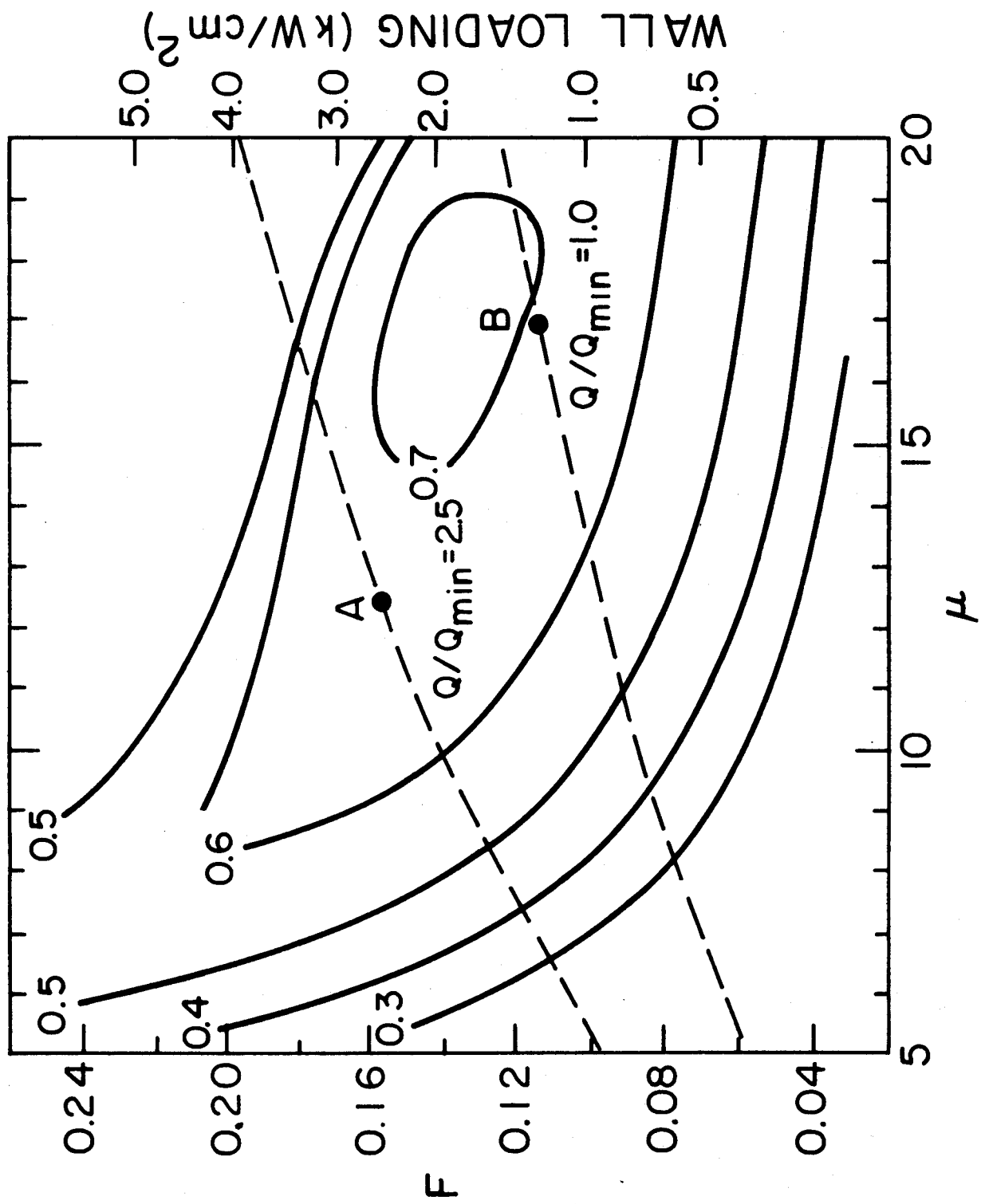


Figure 1

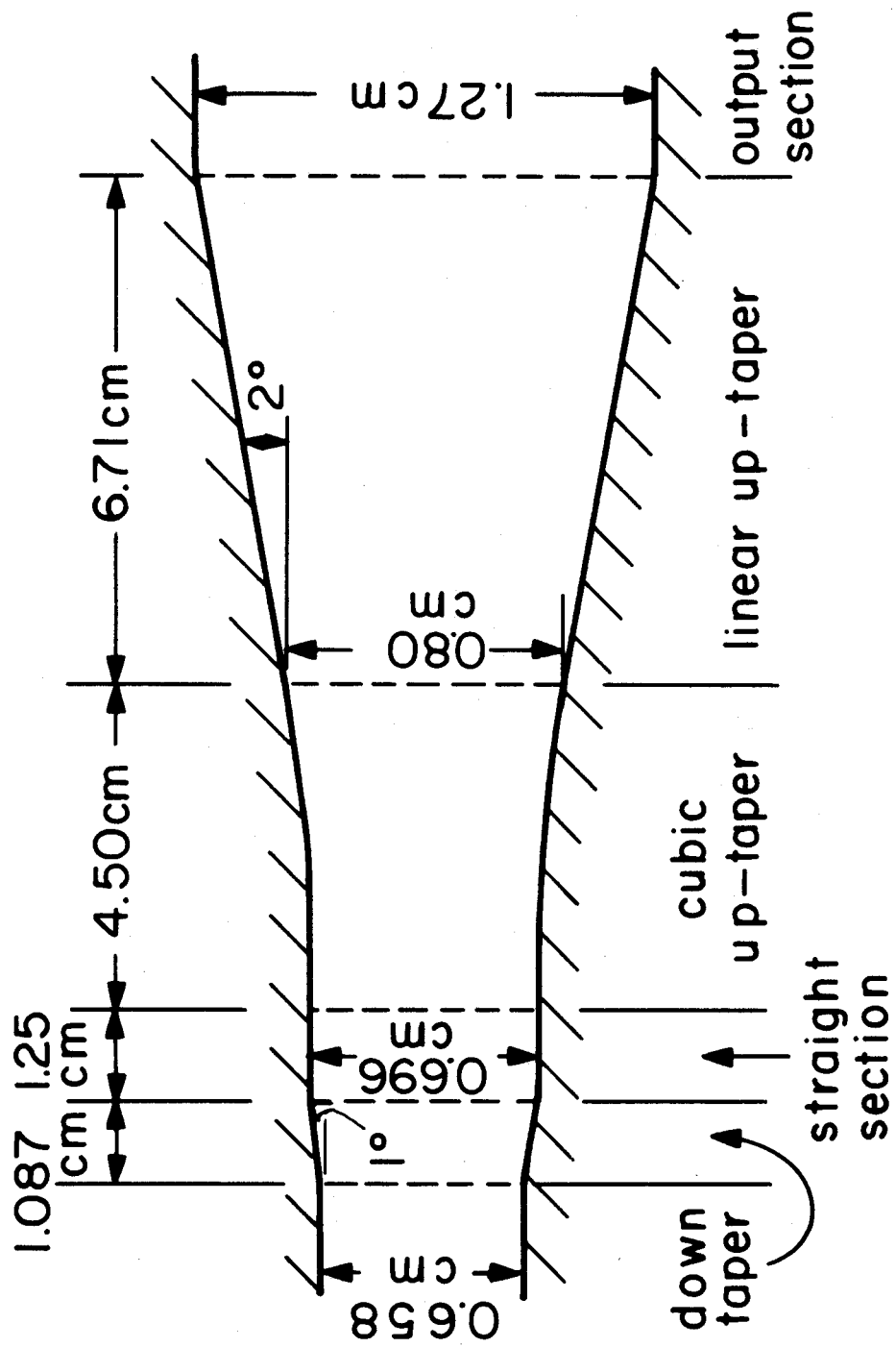


Figure 2

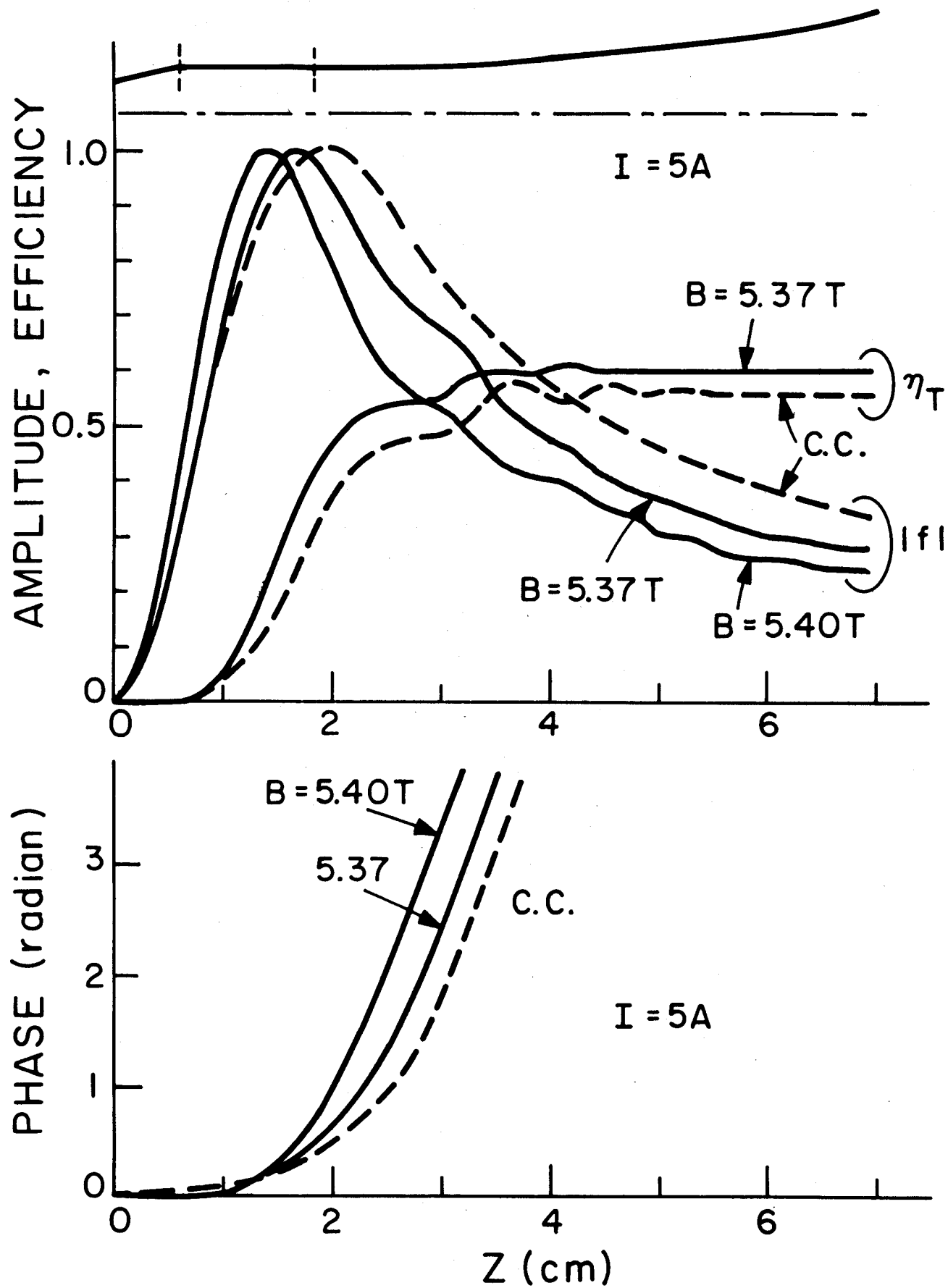


Figure 3

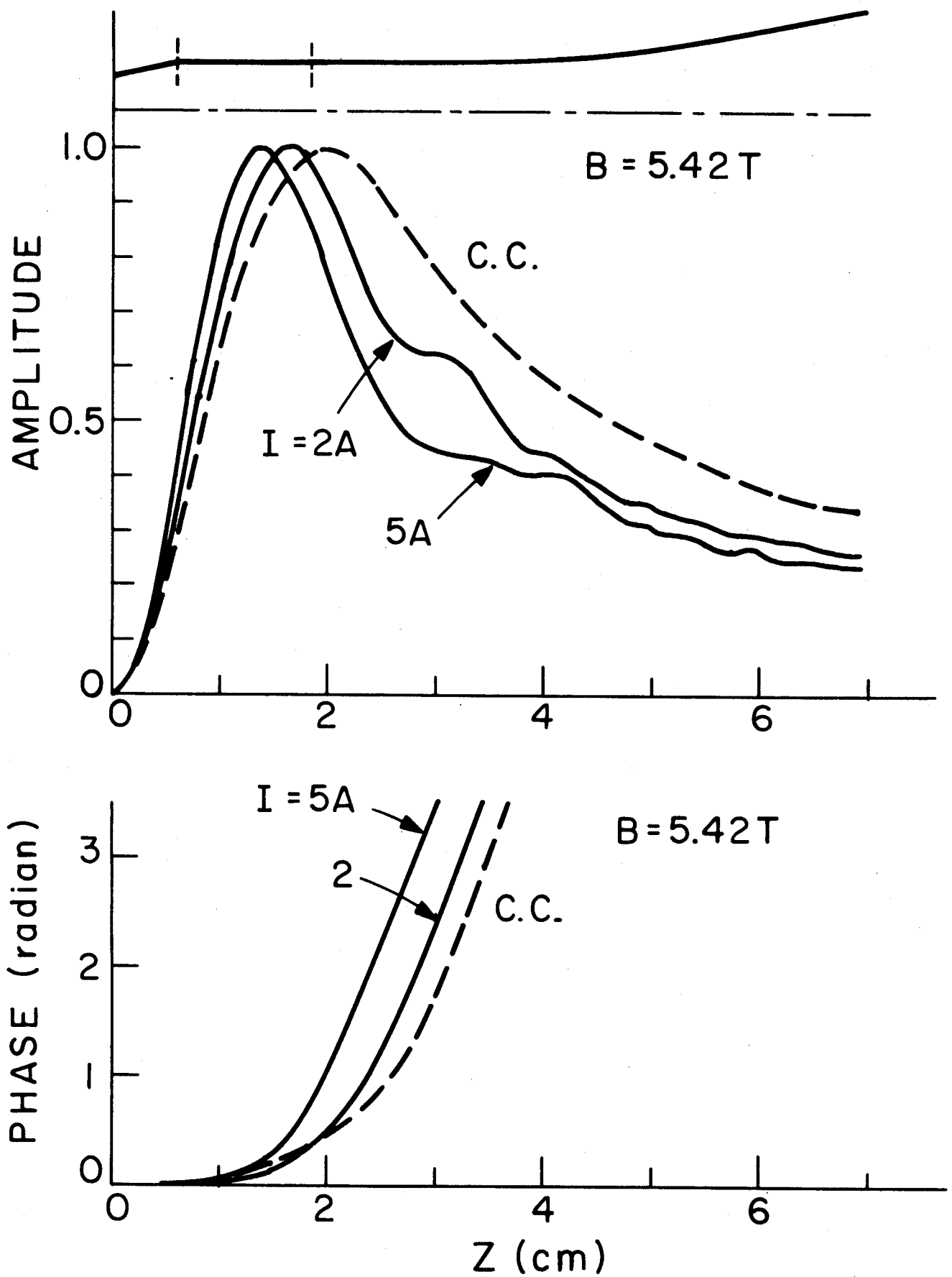


Figure 4

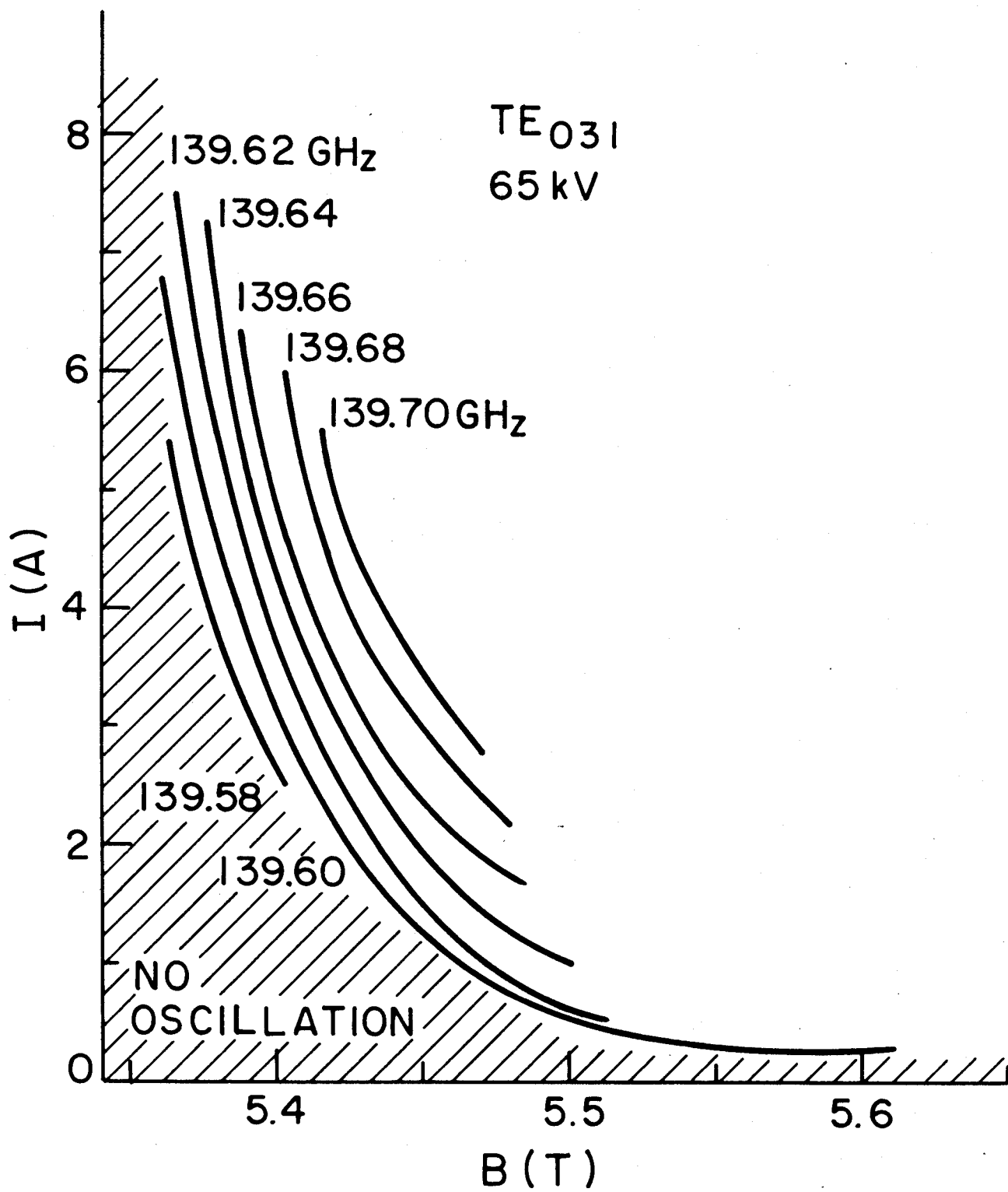


Figure 5

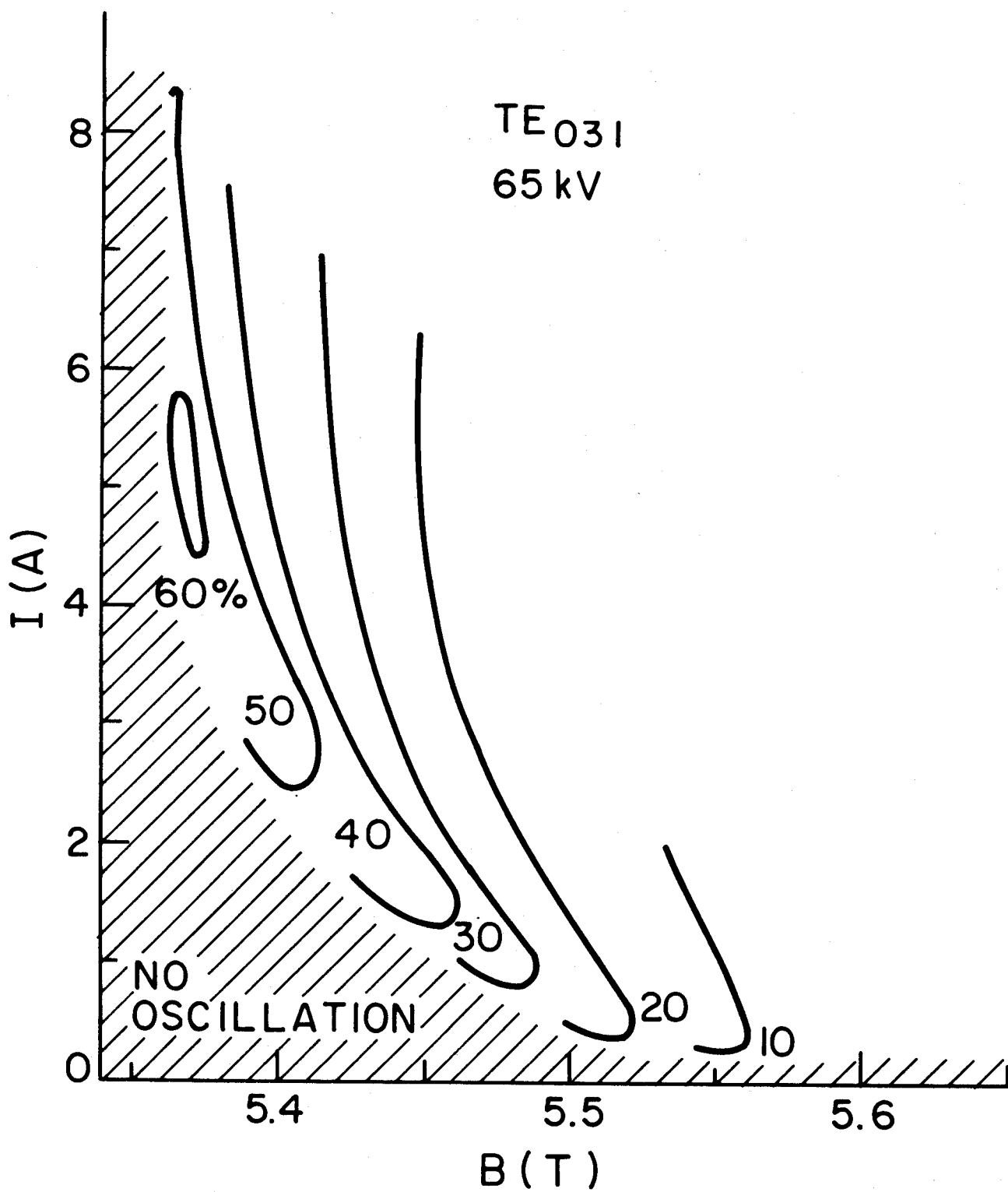


Figure 6

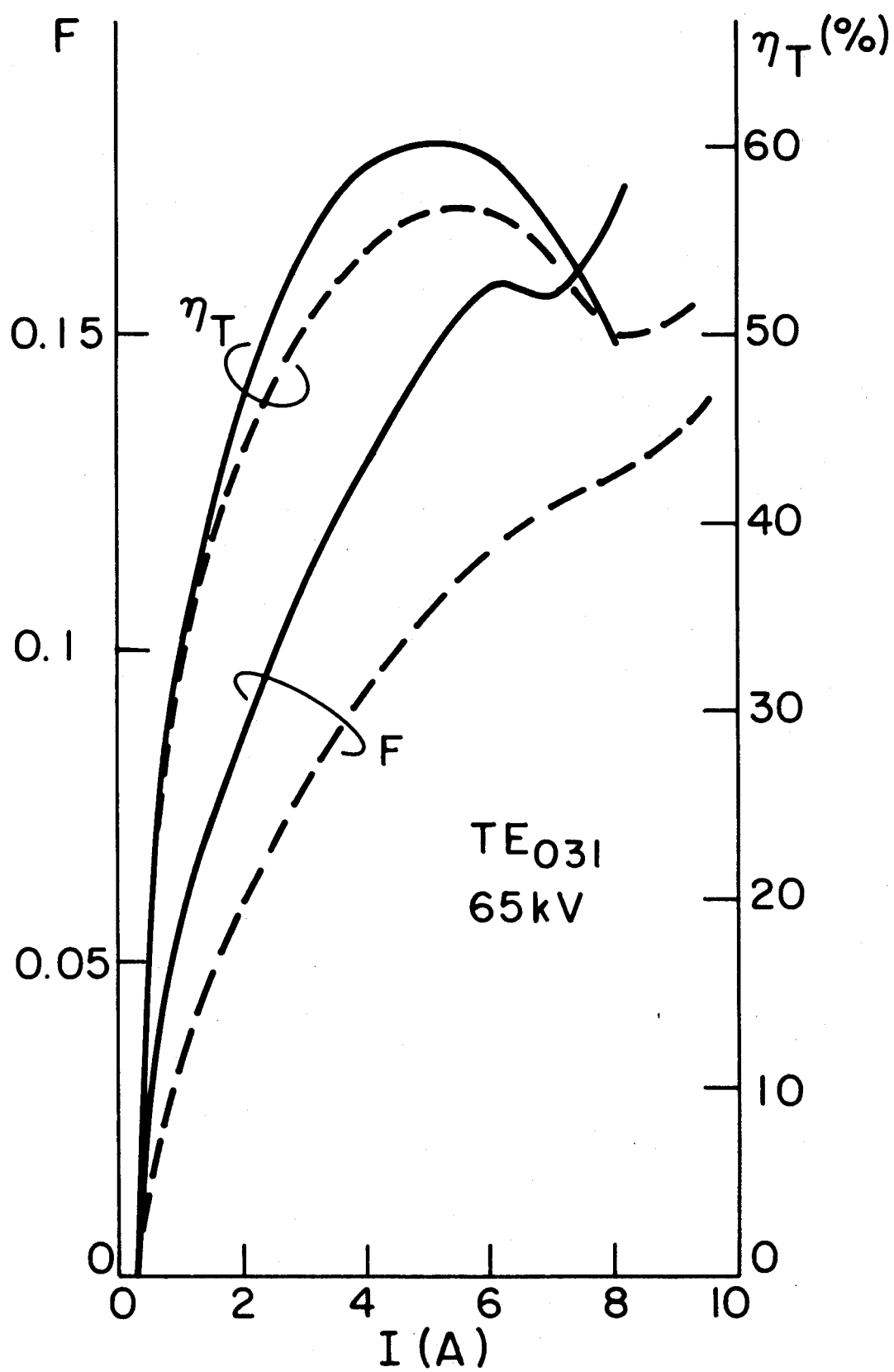


Figure 7

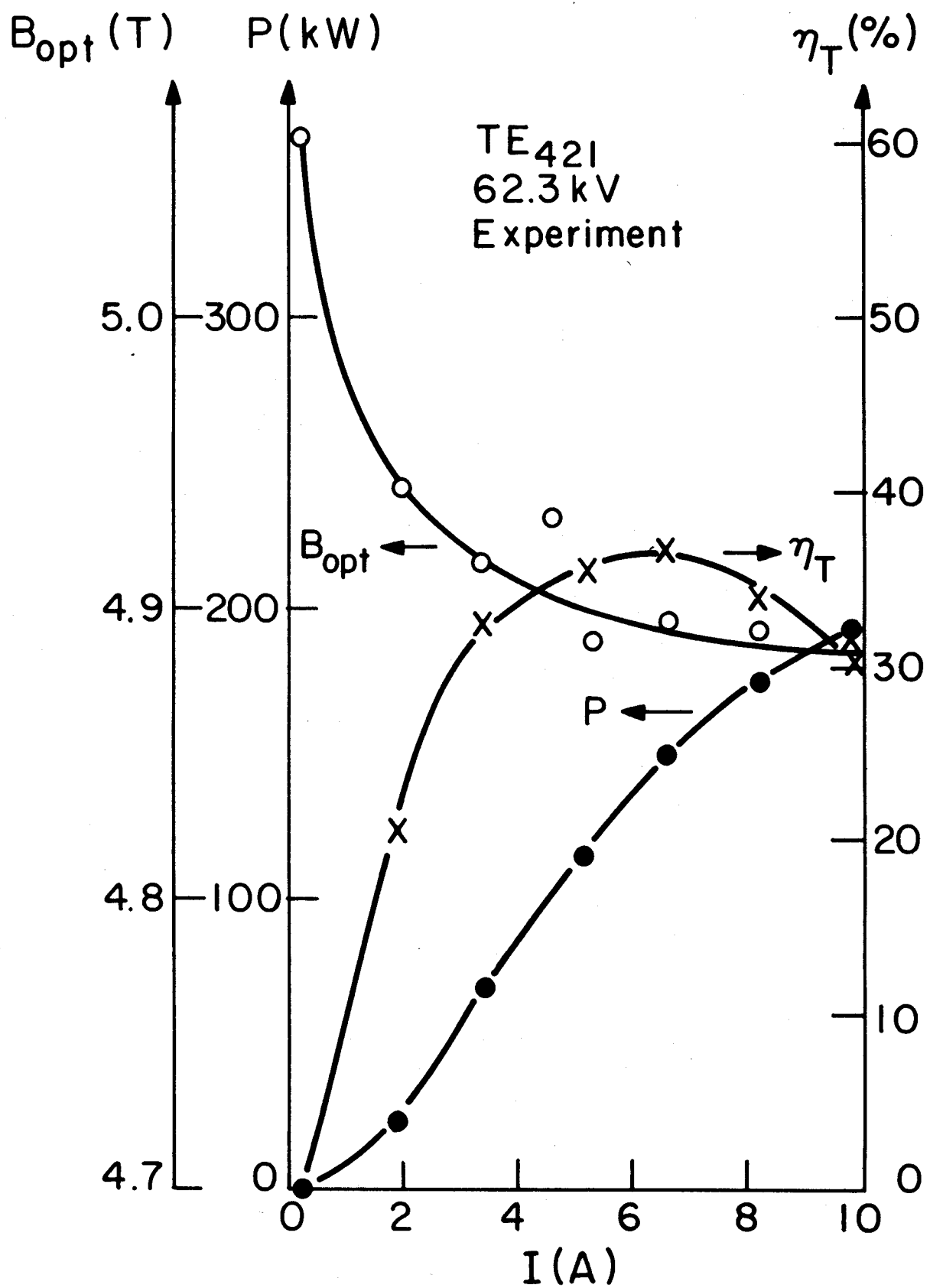


Figure 8

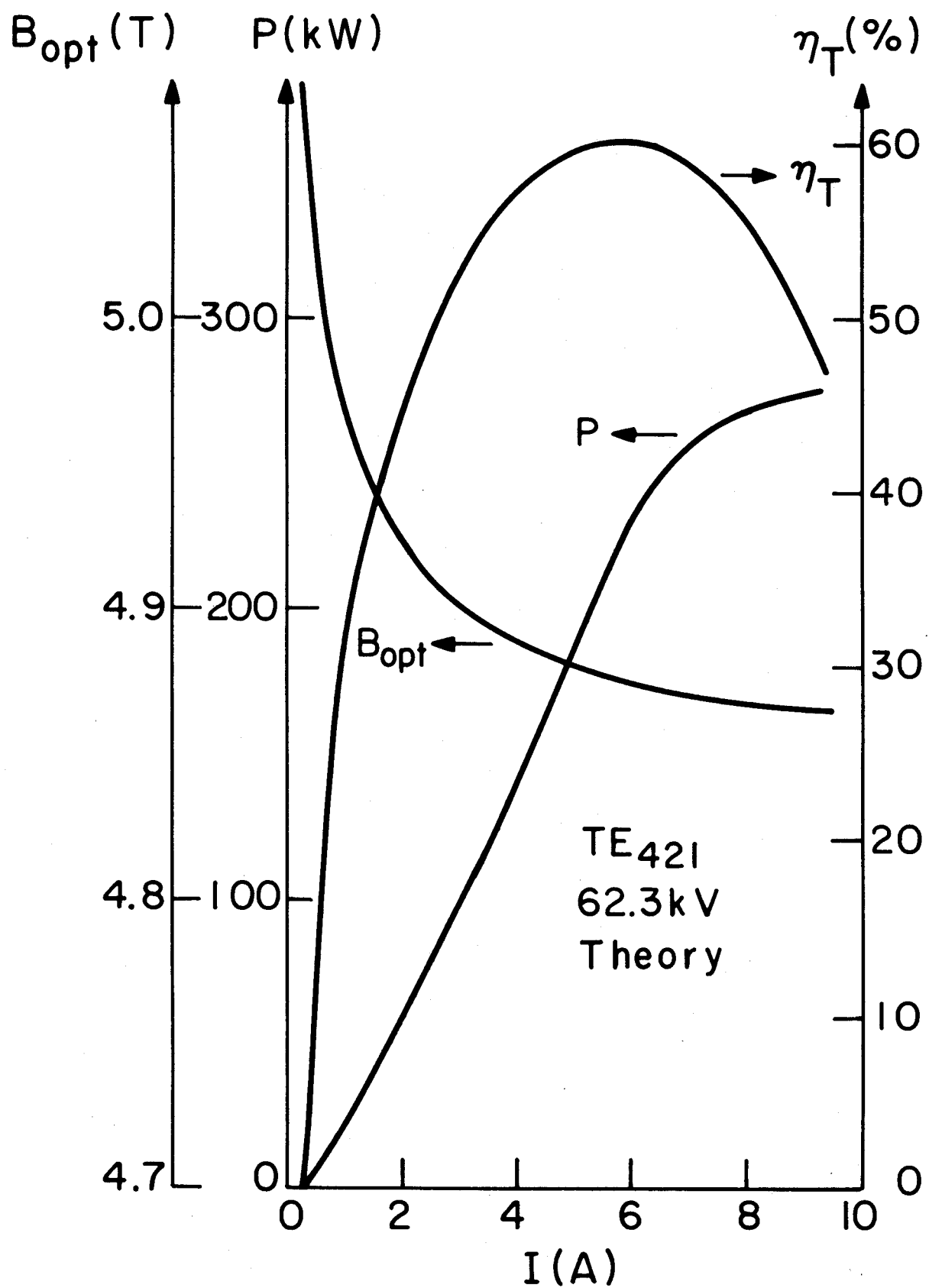


Figure 9

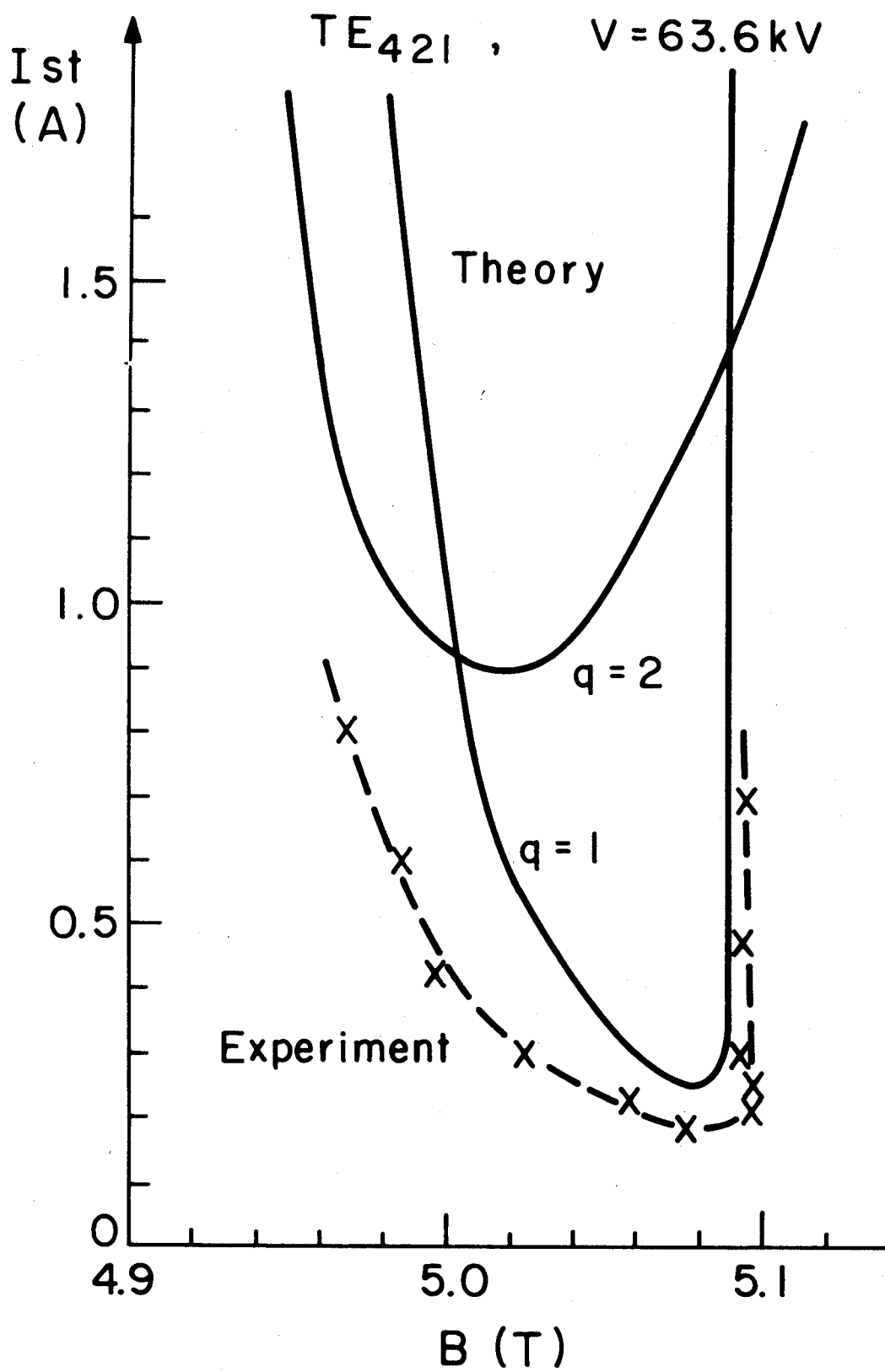


Figure 10

